

**COLOR STUDIES OF THE *CHANG'E-3* LANDING SITE WITH IMAGES FROM THE ROVER PANORAMIC CAMERA.** Tiffanie X. Choi<sup>1</sup>, David T. Blewett<sup>2</sup>, Ashley R. Wang<sup>3</sup>, Yong-Chun Zheng<sup>4</sup>, Edward A. Cloutis<sup>5</sup>. <sup>1</sup>Long Reach High School, Columbia, Md., USA. <sup>2</sup>Planetary Exploration Group, Johns Hopkins University Applied Physics Laboratory, Laurel, Md., USA. <sup>3</sup>River Hill High School, Clarksville, Md., USA. <sup>4</sup>National Astronomical Observatories of Chinese Academy of Sciences, Beijing, China. <sup>5</sup>Dept. of Geography, University of Winnipeg, Canada. (correspondence author: david.blewett@jhuapl.edu).

**Introduction:** The *Chang'E-3* (CE-3) mission placed a lander and rover (*Yutu*) on the lunar surface in Mare Imbrium, at 44.12° N, 340.49° E [1, 2]; touchdown was on 14 December 2013. The rover carried a pair of mast-mounted Panoramic Cameras (PCAM, [3]), used to collect monochrome and color images of the surface during the rover's ~114-m traverse. The PCAM detectors had an array of red-green-blue pixels in the so-called Bayer pattern. The color balance can be adjusted to mimic the sensitivity of the human eye [4], yielding images that have an appearance similar to what a person standing at the landing site would see (Fig. 1A). The CMOS detector produces images with  $2,352 \times 1,728$  pixels when in color mode [5]. Simple manipulations of the three color bands (R-G-B) that make up each image allow for useful analysis. Color ratios (Fig. 1B) are a powerful tool for revealing spectral variations in a scene. Additional analysis can be done by considering the spectral response of the three color filters (Fig. 2), permitting comparisons with reflectance data for returned lunar samples or obtained from lunar orbit.

**Processing PCAM images:** We obtained Level 2B images archived at the National Astronomical Observatories of the Chinese Academy of Sciences website, <http://moon.bao.ac.cn/>. Image reduction to radiance for each pixel includes correction for dark current, flat field, gain, and exposure time [5, 6]. Geometric information for each image includes the solar zenith and azimuth angles, and the platform and camera orientation. We performed demosaicking [7] and converted the R, G, and B image planes to radiance using calibration coefficients contained in the image headers [8]. The radiance images were divided by the solar spectrum [9] convolved to the PCAM responsivities in order to produce images in units of reflectance factor ( $I/F$ ), following the method of Jin et al. (2015) [8]. We then form the three ratios B/R, B/G, and G/R. To first order, spectral ratios normalize photometric differences caused by the widely varying incidence and emergence angles that are typically present within a scene.

**Discussion:** The scene in Fig. 1 includes a columnar-shaped rock, noted by [10]. We defined image regions of interest (ROIs) for the columnar rock, a foreground rock, and a flat patch of foreground soil, shown

as the colored polygons in Fig. 1A. We extracted average three-color reflectance spectra for the ROIs and plotted them along with RELAB spectra for *Apollo* low-Ti mare basalt rocks and soils (Fig. 3). The PCAM spectra were normalized for solar incidence angle relative to a flat surface. A detailed digital elevation map at the scale of this image is not available; hence the absolute reflectance values on Sun-facing facets are likely too high. Nonetheless, it can be seen that the spectral character of the rocks and soils at the site is generally consistent with the spectra of returned samples (Figs. 3 and 4). Detailed examination of extracted spectra and color ratios suggests that the PCAM R-band values are slightly higher relative to the B- and G-bands than expected from the sample spectra; this could be a result of calibration errors or could be caused by real inherent color/compositional differences.

We plan to use the color-ratio images to search for anomalous material that may be present at the landing site, e.g., material excavated from depth within the 450-m crater just west of the site, or remnant impactor material. We will also examine space-weathering trends in the PCAM color data for comparison with spectral maturation relationships as observed from orbit.

**References:** [1] L. Xiao (2014), *Nature Geosci.* 7, 391. [2] L. Xiao et al. (2015), *Science* 347, 1226. [3] J.-F. Yang et al. (2015), *Res. Astron. Astrophys.* 15, 1867. [4] X. Ren et al. (2014), *Res. Astron. Astrophys.* 14, 1557. [5] C. Li et al. (2015), *Space Sci. Rev.* 190, 85. [6] X. Tan (2014), *Res. Astron. Astrophys.* 14, 1682. [7] X. Li (2005), *IEEE Trans. Image Proc.* 14, 370. [8] W. Jin, et al. (2015), *Geophys. Res. Lett.* 42. [9] C. Gueymard (2004), *Solar Energy* 76, 423. [10] A. Basilevsky et al. (2015), *Planet. Space Sci.* 117, 385.

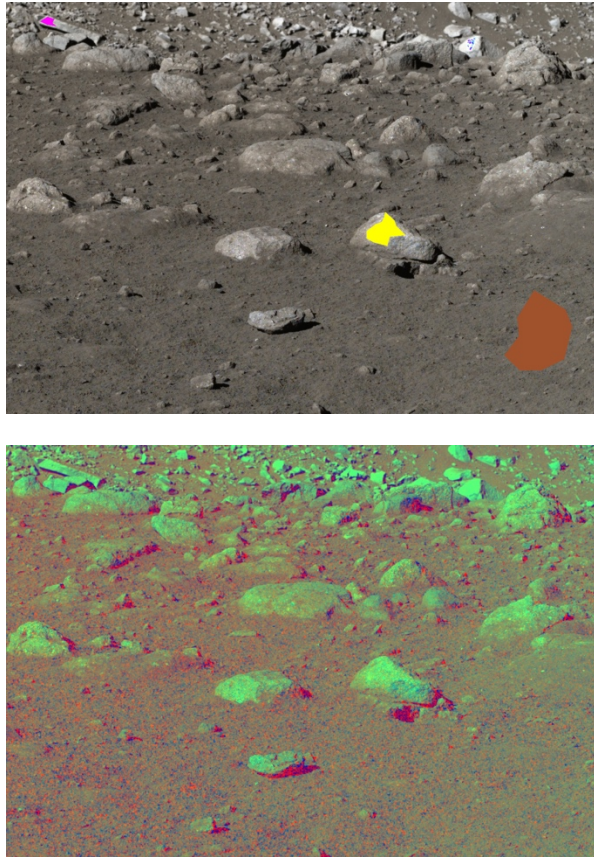


**Fig. 1.** (A) CE-3 PCAM image R\_N20140113191458. Image ROIs were defined for a columnar rock (magenta polygon), foreground rock (yellow), and soil (brown). (B) Color-ratio composite (red channel = R/B, green channel = G, blue channel = B/R), highlighting the reddish nature of the soils relative to the rocks.

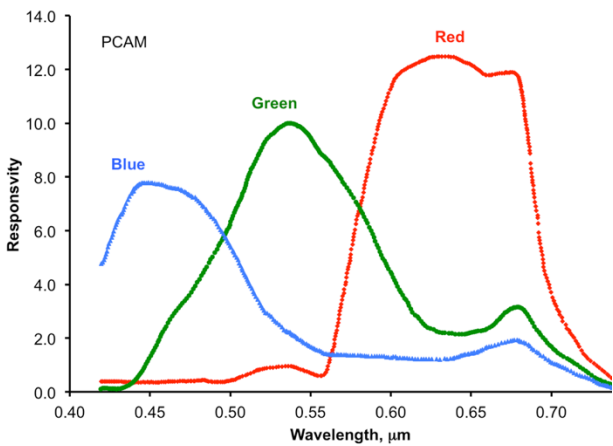


**Fig. 2.** Responsivity of the three PCAM color channels [4].

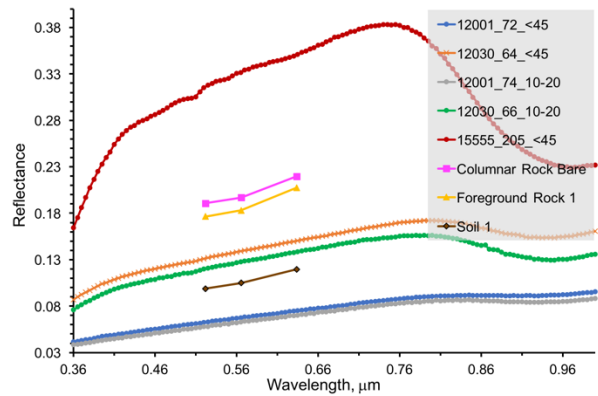


**Fig. 3.** Reflectance spectra for returned lunar samples (RELAB), with average 3-color spectra extracted from the image ROIs shown in Fig. 1A.

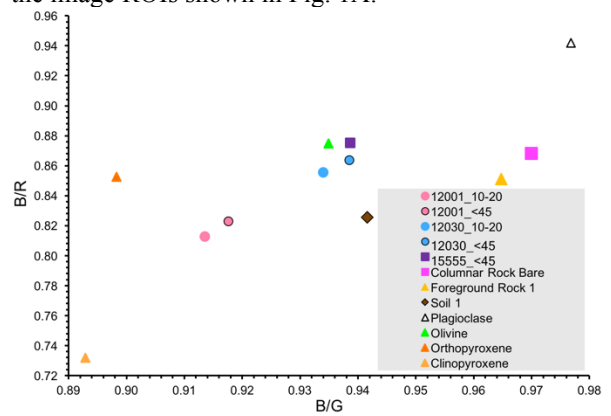


**Fig. 4.** Plot of the B/R ratio vs. B/G ratio for the PCAM ROIs, and for the *Apollo* samples of Fig. 3 convolved to the PCAM responsivities.